4-3

Properties of InAs- and Silicon-Based Ballistic Spin Field-Effect Transistors

Dmitri Osintsev, Viktor Sverdlov, Alexander Makarov, and Siegfried Selberherr
Institute for Microelectronics, TU Wien, Vienna, Austria
{osintsev|sverdlov|makarov|selberherr}@iue.tuwien.ac.at

***Abstract*— We investigate the transport properties of ballistic spin field-effect transistors. The transistor characteristics are examined for a broad range of parameters including the semiconductor channel length, the conduction band mismatch between the channel and the contacts, the strength of the spin-orbit interaction, and the magnetic field. We show that temperature exerts a significant influence on the device characteristics. For the InAs-based transistors a shorter channel is preferred for potential operations at room temperature. For the silicon-based transistors we demonstrate that the [100] fin orientation displays a stronger dependence of the magnetoresistanse on the strength of the spin-orbit interaction and is therefore best suited for practical realization of the silicon spin transistor.**

Spin field-effect transistor, Dresselhaus spin-orbit interaction, tunneling magnetoresistance, temperature

I. INTRODUCTION

With MOSFET scaling rapidly approaching its fundamental limits new engineering solutions have to be developed in order to increase computational speed and decrease power consumption of future integrated circuits. A promising solution is to take into account the carrier spin degree of freedom. Spin of an electron can change its orientation to opposite very fast by using only a dramatically small amount of energy. Thus, utilizing spin properties of carriers opens great opportunity to design devices with superior characteristics which cannot be achieved with the present transistor technology [1].

The spin field-effect transistor (SpinFET) is a switch which employs the spin properties of electrons. The SpinFET is composed of a semiconductor channel region sandwiched between the two ferromagnetic contacts, source and drain. The source contact injects spin-polarized electrons in the semiconductor region. The spin-orbit interaction in the channel is used to modulate the current through the SpinFET [2]. It causes the electron spin to precesses during its propagation through the channel. Only the electrons with their spin aligned to the drain contact magnetization can leave the channel through the drain contact, thus contributing to the current. Importantly, the spin-orbit interaction strength is controlled electrically by applying an external gate voltage.

The total current through the device depends on the relative angle between the magnetization direction of the drain contact and the electron spin polarization at the end of the semiconductor channel. The spin precession angle $\Delta\theta$ defined as the difference between the orientation of the spin of the electron at the end and at the beginning of the semiconductor region is [1]

$$\Delta\theta = \frac{2\alpha\, m^*}{\hbar^2} L, \tag{1}$$

where α is the strength of the spin-orbit interaction, m^* is the effective mass of the electron, $\hbar$ is the reduced Plank constant, and L is the length of the semiconductor channel. The strength of the spin-orbit interaction determines the minimum length of the semiconductor channel, which will be sufficient to alternate the spin orientation.

The two dominant mechanisms of the spin-orbit interaction in well investigated III-V semiconductor heterostructures are of the Rashba and the Dresselhaus type. The Dresselhaus spin-orbit interaction is caused by the bulk inversion symmetry breaking [3], while the Rashba spin-orbit interaction is due to the geometrically induced structural asymmetry [4] in the system. The effective Hamiltonian of the Rashba spin-orbit interaction is in the form

$$H_R = \frac{\alpha_R}{\hbar}(p_x\sigma_y - p_y\sigma_x), \tag{2}$$

where α_R is the effective electric field-dependent parameter of the spin-orbit interaction, $p_{x(y)}$ is the electron momentum projection, and σ_x and σ_y are the Pauli matrices. This is the gate-controlled contribution to the spin-orbit interaction in confined III-V semiconductor devices.

Because silicon is characterized by a weak spin-orbit interaction, it has not been considered as a candidate for the SpinFET channel material. Recently, however, it was shown [5], that thin silicon films in SiGe/Si/SiGe heterostructures can possess large values of spin-orbit interaction. Interestingly, the Rashba spin-orbit interaction in confined silicon structures is relatively weak; its strength is approximately ten times smaller than the value of the dominant

This work is supported by the European Research Council through the grant #247056 MOSILSPIN

978-1-61284-418-3/11/$26.00 © 2011 IEEE

contribution which is of the Dresselhaus type with the corresponding effective Hamiltonian in the form

$$H_D = \frac{\beta}{\hbar}(p_x\sigma_x - p_y\sigma_y), \tag{3}$$

This major contribution to the spin-orbit interaction is due to interfacial-induced disorder which breaks the inversion symmetry. The strength β of the Dresselhaus-like spin-orbit interaction depends almost linearly on the effective electric field, $\beta \cong \beta^1 E_z$, where β^1 is the intra-valley coupling constant [6]. For a field strength of 50kV/cm, the strength of the spin-orbit interaction is found to be β ≈ 2μeVnm [6], which is in agreement with the value reported experimentally [7], while $\alpha_R \approx 0.1$μeVnm. The value of the Dresselhaus spin-orbit interaction in confined silicon structures is sufficient to consider them for application as SpinFET channels.

II. MODEL

To calculate the transport properties of the ballistic spin field-effect transistor we consider a model similar to that of [8], [9]. The Hamiltonian in the ferromagnetic regions has the following form:

$$H = \frac{p_x^2}{2m_f^*} + h_0\sigma_z, \quad x < 0, \tag{4}$$

$$H = \frac{p_x^2}{2m_f^*} \pm h_0\sigma_z, \quad x > L, \tag{5}$$

where m_f^* is the effective mass in the contacts, $h_0=2PE_F/(P^2+1)$ is the exchange splitting energy with P defined as the spin polarization in the ferromagnetic regions, E_F is the Fermi energy, and σ_z is the Pauli matrix; ± in (5) stands for the parallel and anti-parallel configuration of the contact magnetizations. For the InAs semiconductor channel the Hamiltonian is the same as in [8], [9]. For the silicon semiconductor region, the spin-orbit interaction is taken in the Dresselhaus form. The effective Hamiltonian in the channel is

$$H = \frac{p_x^2}{2m_s^*} + \delta E_c + \frac{\beta}{\hbar}\sigma_x p_x + \frac{1}{2} g\mu_B B\sigma^*, \tag{6}$$

where m_s^* is the subband effective mass, δE_c is the band mismatch between the ferromagnetic and the semiconductor region, g is the Landé factor, μ_B is the Bohr magneton, B is the magnetic field, and $\sigma^* \equiv \sigma_x\cos\gamma + \sigma_y\sin\gamma$ with γ defined as the angle between the magnetic field and the transport direction.

To calculate the dependence of the transport properties on the strength of the spin-orbit interaction we take the wave function in the left contact as follows:

$$\Psi_L(x) = (e^{ik_\uparrow x} + R_\uparrow e^{-ik_\uparrow x})\begin{pmatrix}1\\0\end{pmatrix} + R_\downarrow e^{-ik_\downarrow x}\begin{pmatrix}0\\1\end{pmatrix}, \tag{7}$$

$$\Psi_L(x) = R_\uparrow e^{-ik_\uparrow x}\begin{pmatrix}1\\0\end{pmatrix} + (e^{ik_\downarrow x} + R_\downarrow e^{-ik_\downarrow x})\begin{pmatrix}0\\1\end{pmatrix}, \tag{8}$$

where (7) corresponds to the incoming spin-up electrons and (8) to the incoming spin-down electrons, respectively, $k_{\uparrow(\downarrow)} = \sqrt{2m_f^*(E \mp h_0)/\hbar^2}$ is the wave vector of the spin-up (spin-down) electrons, and $R_{\uparrow(\downarrow)}$ is the amplitude of the reflected wave. For the right contact the wave function is given by:

$$\Psi_R(x) = C_\uparrow e^{ik_\uparrow x}\begin{pmatrix}1\\0\end{pmatrix} + C_\downarrow e^{ik_\downarrow x}\begin{pmatrix}0\\1\end{pmatrix}. \tag{9}$$

For the semiconductor region the wave function can be written as:

$$\Psi_S(x) = A_+ e^{ik_{x1}^{(+)}x}\begin{pmatrix}k_1\\1\end{pmatrix} + B_+ e^{ik_{x2}^{(+)}x}\begin{pmatrix}k_2\\1\end{pmatrix}$$
$$A\_ e^{ik_{x1}^{(-)}x}\begin{pmatrix}k_3\\-1\end{pmatrix} + B\_ e^{ik_{x2}^{(-)}x}\begin{pmatrix}k_4\\-1\end{pmatrix}, \tag{10}$$

where $k_{x1(x2)}^{(+)}$ and $k_{x1(x2)}^{(-)}$ are the wave vectors obtained by solving the equations $\frac{\hbar^2 k^2}{2m_s^*} + \delta E_c \pm$
$\pm \sqrt{\left(\frac{Bg\mu_B\cos(\gamma)}{2}\right)^2 + \left(\frac{Bg\mu_B\sin(\gamma)}{2} - \beta k\right)^2} = E$,
respectively.

The coefficients k_1, k_2, k_3, and k_4 are calculated as

$$k_1 = -\frac{i\left(Bg\mu_B\sin(\gamma) - 2\beta k_{x1}^{(+)}\right) - Bg\mu_B\cos(\gamma)}{2\sqrt{\left(\frac{Bg\mu_B\cos(\gamma)}{2}\right)^2 + \left(\frac{Bg\mu_B\sin(\gamma)}{2} - \beta k_{x1}^{(+)}\right)^2}}, \tag{11}$$

$$k_2 = -\frac{i\left(Bg\mu_B\sin(\gamma) - 2\beta k_{x2}^{(+)}\right) - Bg\mu_B\cos(\gamma)}{2\sqrt{\left(\frac{Bg\mu_B\cos(\gamma)}{2}\right)^2 + \left(\frac{Bg\mu_B\sin(\gamma)}{2} - \beta k_{x2}^{(+)}\right)^2}}, \tag{12}$$

$$k_3 = \frac{i\left(Bg\mu_B\sin(\gamma) - 2\beta k_{x1}^{(-)}\right) - Bg\mu_B\cos(\gamma)}{2\sqrt{\left(\frac{Bg\mu_B\cos(\gamma)}{2}\right)^2 + \left(\frac{Bg\mu_B\sin(\gamma)}{2} - \beta k_{x1}^{(-)}\right)^2}}, \tag{13}$$

$$k_4 = \frac{i\left(Bg\mu_B\sin(\gamma) - 2\beta k_{x2}^{(-)}\right) - Bg\mu_B\cos(\gamma)}{2\sqrt{\left(\frac{Bg\mu_B\cos(\gamma)}{2}\right)^2 + \left(\frac{Bg\mu_B\sin(\gamma)}{2} - \beta k_{x2}^{(-)}\right)^2}}. \tag{14}$$

The reflection and transmission coefficients are determined by applying the standard boundary conditions at the ferromagnet/semiconductor interfaces. We compute the current through the device as:

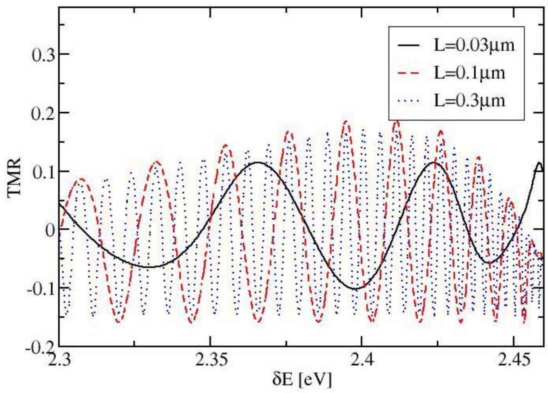

Figure 1. TMR dependence on the value of the δEc for α=31.7meVnm, B=0T, z=0.

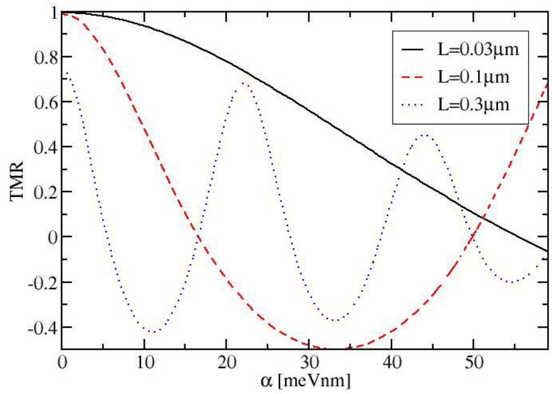

Figure 2. TMR dependence on the value of the Rashba spin-orbit interaction parameter for P=0.6, B=2T, z=5.

$$I^{P(AP)}(V)=\frac{e}{h}\int_{\delta E_c}^{\infty}\left[T_{\uparrow}^{P(AP)}(E)+T_{\downarrow}^{P(AP)}(E)\right] \left\{\frac{1}{1+e^{\frac{E-E_F}{k_BT}}}-\frac{1}{1+e^{\frac{E-E_F+eV}{k_BT}}}\right\}dE, \quad (15)$$

where k_B is the Boltzmann constant, T is the temperature, and V is the voltage. The spin-up ($T^P{}_\uparrow$) and spin-down ($T^P{}_\downarrow$) transmission probability for the parallel configuration of the contact magnetization is defined as:

$$T_{\uparrow}^{P}=\left|C_{\uparrow}\right|^2+\frac{k_{\downarrow}}{k_{\uparrow}}\left|C_{\downarrow}\right|^2, \quad (16)$$

$$T_{\downarrow}^{P}=\frac{k_{\uparrow}}{k_{\downarrow}}\left|C_{\uparrow}\right|^2+\left|C_{\downarrow}\right|^2. \quad (17)$$

For the anti-parallel configuration of contact magnetization the transmission probability is obtained in a similar fashion.

The conductance is defined as:

$$G^{P(AP)}=\lim_{V\to 0}\frac{I^{P(AP)}}{V}. \quad (18)$$

In the limit of low temperatures the conductance must coincide with the one obtained from the Laudauer-Büttiker formula:

$$G^{P(AP)}=\frac{e^2}{h}\left(T_{\uparrow}^{P(AP)}(E_F)+T_{\downarrow}^{P(AP)}(E_F)\right). \quad (19)$$

Finally, the magnetoresistance (TMR) is computed as:

$$TMR\equiv\frac{G^P-G^{AP}}{G^{AP}}. \quad (20)$$

III. Results and Discussion

We first investigate the properties of an InAs ballistic SpinFET. The dominant mechanism of the spin-orbit coupling is due to the geometry-induced inversion symmetry breaking (Rashba type). Figure 1 shows the dependence of the tunneling magnetoresistance on the conduction band mismatch between the ferromagnetic contacts and the channel δE_c. The TMR oscillates between positive and negative values. As expected, for the semiconductor channel of the length L=0.3μ*m* the results are in good agreement to those published by Jiang *et al.*[9]. As the length of the semiconductor channel increases, the period of oscillations decreases approximately proportionally to the length of the semiconductor channel. The dependence of the TMR on the strength of the spin-orbit interaction α is shown in Figure 2. Following [8], [9] the delta-function-like Schottky barriers with a strength $z=2m_fU/\hbar^2k_F$ at the interfaces between the contact and the channel are introduced. With the channel length decreasing less periods of modulation due the spin-orbit interaction are observed. However, even for the length L=0.03μ*m* the modulation of the TMR spans half of the period for the reported spin-orbit interaction values [10], which is sufficient for applications.

Temperature exerts a significant influence on the device characteristics as shown in Figure 3 and Figure 4. For the channel length L=0.3μ*m* the oscillatory amplitude of the TMR dramatically decreases even for $T=10K$ and completely vanishes for $T=77K$. The reason of the oscillatory amplitude vanishing for $T=77K$ is the relatively short period of the oscillations as a function of δE_c. As shown in Figure 1, the period of the oscillations increases proportionally to the channel length. Thus one can expect that for a shorter channel the oscillatory amplitude in δE_c is large enough to modulate the current in the SpinFET even at the room temperature.

The current dependence on the value of the drain-source voltage is shown in Figure 4. A clear S-like shape of the curves is observed at $T=10K$. This is a manifestation of the conductance oscillations as a function of δE_c, which have a large amplitude due to the presence of the delta-function barriers at the interfaces between the contact and the channel (z=3). A large amplitude of the conductance oscillations

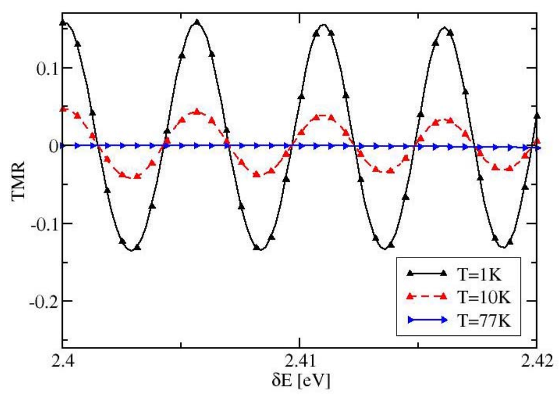

Figure 3. TMR dependence on the value of the δEc for α=31.7meVnm, B=0T, z=0, P=0.4, L=0.3µm.

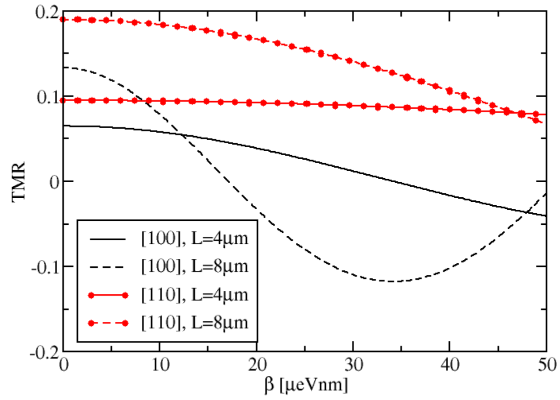

Figure 5. TMR dependence on the value of the Dresselhaus spin-orbit interaction for for E_F=2.47eV, δE_c=2.154eV, P=0.4, z=2.

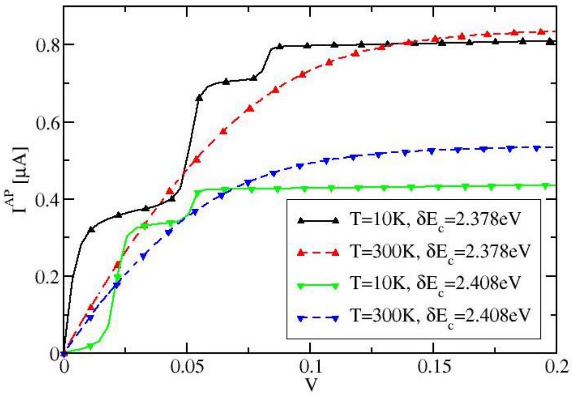

Figure 4. Current dependence on the value of the applied field for B=0T, z=3, L=0.03µm.

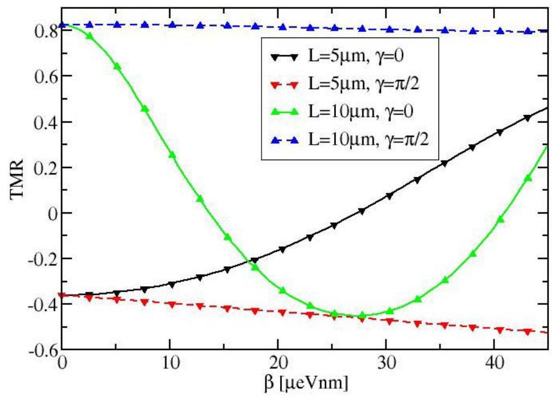

Figure 6. Same as in Figure 5 for B=4T, z=3. γ is the angle between the magnetic field and the transport direction.

guarantees different slopes of the IV curves corresponding to different δE_c. Although the S-like non-linearity is not visible at elevated temperatures, the difference in the slopes at small voltages is not completely washed out at room temperature. Figure 4 also displays that the value of the saturation current depends on δE_c even at room temperature. This provides an option to tune the on-current and thus the performance of a SpinFET.

Finally we study properties of the SpinFET built on silicon. To reduce the spin relaxation we take silicon fins with a square cross section of the channel material. Figure 5 demonstrates the dependence of the TMR on the strength of the spin-orbit interaction. The wave vector $k_D = m_S\beta/\hbar^2$ determines the dependence of the TMR on the value of the strength of the Dresselhaus spin-orbit interaction β. Fins with [100] orientation possess a larger subband effective mass [10], [11] compared to [110] oriented fins. Therefore, a smaller variation of β is required in [100] oriented fins to achieve the same k_D and thus the same variation of the TMR. Because of the Dresselhaus form of the spin-orbit interaction, the TMR of [100] oriented fins is most affected by a magnetic field orthogonal to the transport direction as demonstrated in Figure 6. Therefore, [100] fins are best suited to be used as channels in silicon SpinFETs.

IV. Summary and Conclusion

The transport properties of spin field-effect transistors based on InAs and silicon are investigated in the broad range of parameters. It is demonstrated that for the InAs-based SpinFET with a channel length 0.3 µm the temperature T=77K kills already the ability to modulate the TMR value by changing the bandgap mismatch between the channel and the contacts, and shorter channels is required for operation at elevated temperature. For the silicon-based SpinFET the [100] fin orientation displays a stronger dependence on the value of the spin-orbit interaction and is thus preferred for a practical realization of SpinFETs.

References

[1] S. Sugahara and J. Nitta, *Proceedings of the IEEE*, **98** (2010).
[2] S. Datta and B. Das, *Appl. Phys. Lett.*, **56**, 665 (1990).
[3] G. Dresselhaus, *Phys. Rev.* **100**, pp.580-586 (1955).
[4] E. I. Rashba, *Fiz.Tver. Tela (Solid State Physics USSR)*, **2**, 1109 (1960).
[5] M. Nestoklon *et al., Phys. Rev.*, B **77**, 155328 (2008).
[6] M. Prada *et al., New J.Phys.*, **13**, 013009 (2011).
[7] Z. Wilamowski and W. Jantsch, *Phys. Rev. B*, **69**, 035328 (2004).
[8] M. Cahay and S. Bandyopadhyay, *Phys. Rev. B*, **69**, 045303 (2004).
[9] K. Jiang *et al.*, *IEEE T- ED,* **57**, 2005 (2010).
[10] H. Tsuchiya *et al.*, *IEEE T- ED,* **57**, 406 (2010).
[11] D. Osintsev *et al.*, *Proc. 219 ECS Meeting*, **35**, 277 (2011).